On the Regeneration of Fish Scales: Structure and Mechanical Behavior

S. Ghods[1], S. Waddell[1], E. Weller[1], C. Renteria[1], H.-Y. Jiang[1,2], J.M. Janak[3], S.S. Mao[4], T.J. Linley[3,♠], and D. Arola[1,4,5,♠]

[1]Department of Materials Science and Engineering, University of Washington, Seattle, WA USA
[2]Department of Mechanics, Southeast University, Nanjing, China
[3] Pacific Northwest National Laboratory, Richland, Washington,
[4]Shanghai Institute of Applied Mathematics and Mechanics, School of Mechanics and Engineering Science, Shanghai University, Shanghai, China
[5]Department of Mechanical Engineering, University of Washington Seattle, WA USA

The authors have no conflict to declare.

♠Corresponding Authors

Dwayne D. Arola, Ph.D.
Department of Materials Science and Engineering
University of Washington
Roberts Hall, 333
Box 352120
Seattle, WA 98195-2120
darola@uw.edu

T.J. Linley, Ph.D.
Aquatic Research Laboratory
Pacific Northwest National Laboratory
PO Box 999
Richland, WA 99352
Timothy.Linley@pnnl.gov

Abstract –

Fish scales serve as a dermal armor that provides protection from physical injury. Due to a number of outstanding properties, fish scales are inspiring new concepts for layered engineered materials and next-generation flexible armors. While past efforts have primarily focused on the structure and mechanical behavior of ontogenetic scales, the structure-property relationships of regenerated scales have received limited attention. In the present study, common carp (*Cyprinus carpio)* acquired from the wild were held live in an aquatic laboratory at 10° and 20°C. Ontogenetic scales were extracted from the fish for analysis, as well as regenerated scales after approximately 1 year of development and growth. Their microstructure was characterized using microscopy and Raman spectroscopy, and the mechanical properties were evaluated in uniaxial tension to failure under hydrated conditions. The strength, strain to fracture and toughness of the regenerated scales were significantly lower than those of ontogenetic scales from the same fish, regardless of the water temperature. Scales that regenerated at 20°C exhibited significantly higher strength, strain to fracture and toughness than those regenerated at 10°C. The regenerated scales exhibited a highly mineralized outer layer, but no distinct limiting layer or external elasmodine; they also possessed a significantly lower number of plies in the basal layer than in the ontogenetic scales. The results suggest that a mineralized layer develops preferentially during scale regeneration with the topology needed for protection, prior to the development of other qualities.

Keywords: collagen, fish, natural armor, regeneration, scales, toughness

Introduction

Dermal armors are a special class of structural tissues that serve a variety of functions and exhibit a wide range of mechanical properties. These tissues have been modified extensively in response to both biotic and abiotic selection pressures (Weiner and Addadi, 1997; Barthelat, 2007; Meyers, 2012), primarily through differences in mineral content and microstructure array (Currey, 1999; Meyers et al., 2008; Zhang et al., 2011). As a result, many dermal armors possess exceptional mechanical qualities, such as high strength and toughness to weight ratios and resistance to damage. Although armors such as highly mineralized shells primarily function to prevent or reduce predatory injury, other tissues such as fish scales, that are both tough and flexible, have also evolved to facilitate locomotion (Yang et al., 2013).

The scales of modern fish have evolved into four primary groups: cosmoid, placoid, ganoid and elasmoid (Kardong, 2006; Sire and Huysseune, 2003). Elasmoid scales have been of particular interest because they are often found on fish of high mobility requiring significant bending movement of their bodies. As such, the need for flexibility has imposed additional design requirements on scale architecture and composition (Webb, 1983; Szewciw et al., 2017). Like many biological materials, elasmoid scales possess a hierarchical microstructure that has been identified to play a key role in their mechanical properties (Khayer Dastjerdi and Bathelat, 2015; Zhu et al., 2012). Across its thickness, the elasmoid scale can be divided into two principle layers (Figure 1) – the exterior limiting layer and the underlying elasmodine (Arola et al., 2018). The limiting layer is essentially a coating of calcium-deficient apatite reinforced with a sparse distribution of collagen fibers. The elasmodine consists of lamina (or plies) of unidirectional collagen fibrils arranged with a Bouligand helical stacking sequence (Bigi et al., 2001; Ikoma, 2003; Murcia et al., 2017; Torres et al., 2008; Zimmerman et al., 2013). The elasmodine can be

further separated into external and the internal sub-layers differentiated by their relative mineral content. Collagen fibrils of the external elasmodine are more highly mineralized with nanocrystals of apatite; the degree of mineralization is most dense closest to the limiting layer, and then decreases to the internal elasmodine (Gil Duran et al., 2016; Murcia et al., 2016). Correspondingly, there is a gradient in the hardness and elastic modulus through the scale thickness (Chen et al., 2012; Meyers et al., 2012; Arola et al., 2018).

Within the last decade, elasmoid fish scales have attracted substantial interest. Most efforts have evaluated the mechanical behavior of scales under uniaxial tension, transverse puncture, and impact (Marino Cugno Garrano et al., 2012; Zhu et al., 2013, Yang et al., 2014; Torres et al., 2015). Recent investigations within our group have explored the effects of changes in intermolecular bonds stimulated by polar solvents on scale properties (Arola et al., 2019; Murcia et al., 2016). Collectively, these investigations are helping to develop an understanding of their unique microstructure and structure-property relationships. However, these studies have been largely comparative in nature and constrained to analysis of ontogenetic scales obtained from fish at sacrifice, with limited knowledge of the environment in which the scales developed.

When fish scales are lost or damaged, they undergo rapid regeneration through growth and mineralization to restore protective function, which places a high demand on calcium mobilization from internal and external sources (Takagi et al., 1989; Bereiter-Hahn and Zylberberg, 1993). The structure-property relationships of regenerated scales may be highly relevant to this process. To our knowledge, no study has been reported on the mechanics of regenerated scales, or how environmental conditions influence these relationships. Water temperature, for example, has a direct effect on both scale growth and mineral composition (Gauldie et al., 1990; Beakes et al.,

2014; Thomas et al., 2019) and we hypothesized it might have a similar influence on the mechanical properties associated with these processes.

In this investigation the microstructure and mechanical behavior of ontogenetic and regenerated scales from Common carp (*Cyprinus carpio)* are compared. The species has been distributed throughout the world by introduction into natural waters and from cultivation as a food fish (Kloskowski, 2011) and can tolerate temperatures over a range of approximately 2-30 ºC (Panek, 1987). The differences in scale properties are discussed as a function of the water temperature in which they regenerated, as well as the importance of these qualities to their performance for protective function.

Materials and Methods

Common carp (*Cyprinus carpio*) were captured in a flood plain channel adjacent to the Yakima River in southeastern Washington in July 2016. The fish (n=15) were caught with a beach seine net (25m x 3m) and transported in an 800 L insulated tank supplied with oxygen to the Pacific Northwest National Laboratory (PNNL) where they were transferred into a 2000 L holding tank supplied with ambient temperature water (~ 17 °C at time of capture) from the Columbia River at a rate of 100 L/min. Then in March 2017, six fish were selected based on uniformity in body size and condition, placed into two additional 2000 L tanks (n=3 fish per tank) and acclimated to the two experimental temperatures by slowly increasing the ambient water temperature from approximately 6 °C to 10 °C and 20 °C over a period of 7 days. We used late March as the starting point for the experimental treatments because it represents the time when the ambient water temperature in the Columbia River begins to increase following the annual minimum in early to mid-February (Figure 2a), and thus consistent with the temperature cycle the fish would experience

under natural conditions. The experimental temperatures of 10 °C and 20 °C were chosen because they are near the mid-point of the range of temperatures (~ 2-30 ºC) that *C. carpio* occupy throughout their natural environment of (Panek, 1987) and encounter seasonally in the Columbia River (Figure 2a). Under artificial culture conditions with *ad libitum* diet these temperatures provide maximum somatic growth rates of approximately 0.7 and 3% body weight per day, respectively (Goolish and Adleman, 1984). However, because scale growth is also highly dependent on temperature and feeding rate (Beakes et al., 2013), the fish were fed a commercial diet (Pond LE, Skretting, USA) at a rate approximating a maintenance ration (0.5 and 1.0% body mass per day at 10 °C and 20 °C, respectively) to minimize any confounding effect of somatic growth on scale growth. Prior to transfer the fish were weighed, measured for length and tagged with a passive integrated transponder (PIT) for individual identification. These six fish had a mean (± standard deviation) length and mass of 59.7 cm ± 5.2 and 4.2 kg mass ± 1.1, respectively.

In August and September 2017, the first set of ontogenetic scales (n=5 per fish) were extracted from three fish each held at 10°C and 20°C. Prior to extracting the scales, the fish were anesthetized by immersion in a solution of tricaine methanesulfonate (MS-222) at a concentration of 80 mg/L, after which the scales were removed with forceps. The fish were then returned to their respective experimental tanks and allowed to recover from the anesthesia. The scales were taken along two adjacent rows on the right side of each fish in the area immediately behind the gill plate and above the lateral line as shown in Figure 2b. Each ontogenetic scale was visually examined to ensure it had not been regenerated from prior loss of the scale at that site. These could be identified upon removal by a diffuse focus and irregularly formed circuli (Bereiter-Hahn and Zylberberg, 1993). In August of 2018, regenerated scales (n=5 per fish) were collected from the three carp held at 10°C and at 20°C. The regenerated scales were obtained from the same sites as the ontogenetic

scales extracted in 2017. Regenerated scales were easy to discern externally because they lacked the pigmentation present in ontogenetic scales, and because each fish was photographed after scale removal to identify the specific collection sites. These can be seen as lighter colored sites in Figure 2b. At the same time an additional n=5 ontogenetic scales per fish were sampled from the area immediately behind the location of the regenerated scales (Fig. 2a). All of the extracted scales were placed in Hanks Balanced Salt Solution (HBSS) and stored at 3-5 °C until shipment to the University of Washington (less than one month). The capture, care and experimental procedures performed on the fish used in this study were performed under the PNNL Animal Care and Use Committee protocol 2017-02.

All the ontogenetic and regenerated scales possessed a diameter between 1 to 2 cm and were less than 1 mm thick. Due to their limited size, we utilized a specimen geometry that accommodated the tissue available from the scales. Conventional dog-bone shaped tensile specimens were sectioned from the scales with dedicated punch and stamping process to enable an evaluation of the tensile properties (Marino Cugno Garrano et al., 2012). A single specimen was stamped from the central area of each scale where the thickness was most uniform, with a gage section length and width of 5.5 mm and 1.5 mm, respectively (Fig. 2b). The remaining portion of the scales were retained for further analysis. Due to the potential for anisotropic mechanical behavior of scales from the head region (Murcia et al., 2015), all the specimens were obtained with alignment parallel to the fish length, for consistency. After sectioning, all specimens were placed in a bath of HBSS for a minimum of 24 hours. Four specimens were obtained from four separate ontogenetic and regenerated scales in each fish to produce a total of 48 tensile tests overall (2 growth conditions x 4 specimens per fish x 3 fish per temperature x 2 temperatures = 48).

Tensile testing of the fish scale specimens was performed to failure at room temperature and with hydration. The evaluation was conducted using a commercial universal testing machine (Instron ElectroPuls E1000, Norwood, MA, USA) equipped with load cell having full-scale range of 250 N and load precision of 0.01%. The specimens were removed from the HBSS bath, mounted in the grips, and testing was conducted immediately in air. An eyedropper was used to apply HBSS over the duration of the tests to prevent dehydration. Loading was performed under displacement control at a quasi-static strain rate of 10^{-3} s^{-1} up to failure. Though these scales are known to be highly strain rate dependent (Ghods et al., 2019), the quasi-static strain rate was chosen to be consistent with prior studies (Yang et al., 2014; Zhu et al., 2012). Failure of the specimens always occurred within the gauge section. The load and displacement data obtained from the tension tests were used with the measures of the specimen gage section dimensions (average thickness and width measured across three points of the gauge section using a pair of digital calipers) to obtain the engineering stress-strain responses. These curves were used to estimate the elastic modulus (E), strength (S), strain at failure (e_f), and modulus of toughness (MOT). The elastic modulus was determined using the secant method for strains less than 1% and the strength was defined by the maximum stress realized by the sample up to failure. The MOT was calculated by integrating the area under the stress-strain curves as a function of strain until failure.

An evaluation of the microstructure was performed on the scales of all the fish involved in this investigation to understand the differences between the ontogenetic and regenerated scales, as well as the influence of water temperature on scale growth and structure. For this purpose, the remnants of scales used for the tensile specimens were also utilized for imaging and evaluation of the chemical composition. The part of the scale most adjacent to the tensile specimen gauge section was separated from the remainder of the scale, treated using an ascending ethanol treatment and

then mounted in an epoxy compound for polishing and analysis. After mounting, the samples were polished with SiC abrasive paper from mesh numbers of #800 to #4000. Final polishing was performed with a diamond liquid suspension of 1 micron, followed by a liquid suspension of 0.3micron alumina. The polished samples were imaged using an optical microscope (Olympus BX50 Microscope, Olympus Scientific Solutions America, Waltham, MA, USA). The cross-section of the scales was evaluated in terms of the thicknesses of the principle layers, the number of plies in the elasmodine, and any general changes in the scale morphology that could be identified.

To further understand contributions from the microstructure to the mechanical behavior, an analysis of the chemical composition was performed on selected scales using Raman spectroscopy (Renishaw InVia, West Dun-dee, IL, USA). Specifically, scans were performed on three randomly selected ontogenetic and regenerated scales from each fish to obtain measures of the mineral to collagen ratio across the scale thickness, and as a function of distance from the scale's exterior surface. The scans were performed over the spectral range of 400 to 1800 cm^{-1} with a Raman fluorescence microscope (50X objective; Leica, Buffalo Grove, IL), resolution of 10 x 50 µm, laser wavelength of 785 nm and an acquisition time of 10 sec. The spectrum was acquired starting from the scale exterior continuing to the interior in increments of either 6 µm or 12 µm for the regenerated and ontogenetic scales, respectively. The acquired Raman spectra were baseline corrected using commercial software (WiRE 3.4, Renishaw, West Dun-dee, IL, USA) to account for fluorescence.

The mineral to collagen ratio of regions of interest of the scales was calculated using the Raman spectra from the area ratio of the phosphate (961 cm^{-1}) and amide I (1690 cm^{-1}) peaks, following previously established methods [Arola et al. 2018]. A representative Raman spectrum

of a fish scale from this study with annotation of the mineral (i.e. phosphate) and collagen (i.e. amide I) peaks is shown in Figure 2c. Measures of the thickness of the highly mineralized layer were obtained from the spatial variations in the spectra, as well as the chemical composition. Differences in the mineral to collagen ratio and composition of the regions of importance were compared as a function of distance from the limiting layer.

To test for significance, the mechanical properties, microstructural measurements and results from Raman spectroscopy were compared using a Repeated Measures Two-Way Analysis of Variance (ANOVA); $p \leq 0.05$ was used to identify significance. This method of statistical analysis accounts for the between fish variance while showing the significance in the properties of the scales between conditions. All data acquired in this investigation are available at request from the corresponding author.

Results

Micrographs of representative ontogenetic and regenerated scales from fish held at 10°C and 20°C are shown in Figure 1. The microstructure of the ontogenetic scales was consistent with that reported in earlier investigations of scales from common carp with well-defined limiting layer, including external and internal elasmodine regions [Murcia et al., 2018]. By contrast, regenerated scales exhibited only two distinct layers, namely a relatively thick mineralized layer and a basal layer as evident in Figure 1(b) and 1(d). The mineral layer of the regenerated scales appeared as a single heavily mineralized region, with no clearly defined sub-layers or plies that would be considered the external elasmodine. The basal layer consisted of a relatively small number of plies and single distribution, with no clear transition between a low and more highly mineralized region. The mean ± standard error in ply thickness of the regenerated scale was 10 μm ± 0.6 compared to

values of 11 μm ± 0.7 and 7 μm ± 0.3 in the external and internal elasmodine, respectively, of the ontogenetic scales.

Measures of the scale morphology, including the layer thicknesses and the number of plies in each layer, are presented in Table 1. The regenerated scales were approximately half of the total thickness and significantly thinner than the ontogenetic scales from the same fish ($p \leq 0.001$). A comparison of the mineralized (limiting layer + external elasmodine vs mineralized layer) and non-mineralized (internal elasmodine vs basal layer) layers of the two groups showed that the mineralized layer exhibited the largest difference in the thickness between the ontogenetic and regenerated scales; the mineralized layers of the ontogenetic scales were approximately 3X thicker than in the regenerated scales ($p \leq 0.001$). By contrast, although the thickness of scales regenerated at 20°C was approximately 30% greater than those regenerated at 10°C, there was no significant difference between the two groups ($p=0.052$). Similarly, whereas regenerated scales had significantly fewer plies than the ontogenetic scales of the same fish, regardless of the aquatic environment temperature ($p \leq 0.001$), there was no significant difference in the number of plies between scales regenerated at 10° and 20°C ($p=0.40$).

Representative stress-strain curves from the tension tests performed on scales from two selected fish are shown in Figure 3. There was a high degree of consistency in the stress-strain responses among the multiple scales at both temperatures. The ontogenetic scales appeared to exhibit superior structural behavior with substantially higher tensile strength (S) and modulus of toughness (MOT). This quality was most evident from the scales of fish held at 10°C (Figure 3a). By comparison, the elastic modulus (E), S and MOT of the regenerated scales were lower than those values for the ontogenetic scales, which again was most evident in the scales regenerated at 10°C (Figure 3b).

The results for the measures of E, S, MOT and strain to failure (e_f) from the stress-strain responses for the scales of fish held at 10°C are shown in Figure 4. The properties of the scales are presented in terms of the average ± standard deviation for the three different fish that were held at this temperature, corresponding to identifications Fish A, B, and C. As evident from these comparisons there was some variation in properties of the scales obtained from each fish. The coefficient of variation (COV) range for stress-strain responses of the ontogenetic and regenerated scales ranged from 0.09-0.21 and 0.13-0.32, respectively. The largest COV overall was in the MOT, although this was minor when compared to the differences between properties of the ontogenetic and the regenerated scales, which were highly significant ($p \leq 0.01$), except for that in the measures of strain to failure being slightly less significant ($p \leq 0.05$). For all the metrics of performance, the regenerated scales exhibited inferior properties with respect to the ontogenetic scales, with the largest differences occurring in S (60%) and the MOT (70%).

Comparisons of E, S, e_f, and MOT of the ontogenetic and regenerated scales from the fish maintained at 20°C are shown in Figure 5. Consistent with the data presented in Figure 4, these properties are shown individually for scales of three different fish with individual identification numbers D, E, and F. The ranges in the COV for E, S, e_f, and MOT were 0.13-0.18 and 0.08-0.28, respectively, for the ontogenetic and regenerated scales, which were similar in variance to results for the fish held at 10°C. Although S, e_f, and MOT of the regenerated scales were lower than in the ontogenetic scales, the extent of these differences were less than for scales regenerated at 10°C. Surprisingly, E of the regenerated scales for Fish F was nearly 50% higher than that of the ontogenetic scales (Figure 5a). Yet, there was no significant difference in the overall mean E of the ontogenetic and regenerated scales when all of the scales from the fish held at 20°C were included ($p=0.27$). However, the differences in all other mechanical properties between the

ontogenetic and regenerated scales were significantly different ($p \leq 0.05$) with the largest difference represented in the MOT (40%). Temperature related effects on the mechanical properties of the regenerated scales were also present. Elastic modulus, S and MOT were all significantly lower in scales regenerated at 10°C than at 20°C ($p < 0.001$), whereas the e_f was not ($p = 0.145$).

Raman spectroscopy revealed clear differences in the relative degree of mineralization among the distinct structural layers in the ontogenetic and regenerated scales. These differences can be seen from the spectra of the mineral to collagen ratio across the thickness of selected scales from fish held at 10°C (Figure 6). For the ontogenetic scale (Figure 6a), the mineral to collagen ratio was maximum within the limiting layer, and then underwent a marked reduction at the transition of the limiting layer/external elasmodine interface, and again at the external/internal elasmodine interface. In the regenerated scale (Figure 6b), the highest mineral/collagen ratio was present in the outermost thick mineral layer of the scale, which was lower than the limiting layer from the ontogenetic scale but similar to that of the external elasmodine. There was a decrease in mineral to collagen ratio at the transition to the basal layer, and then a further decline through the thickness analogous to trends identified in the internal elasmodine for the ontogenetic scales.

Area ratios of the phosphate and amide I peaks used to quantify the extent of mineralization through the cross-sections of the scales as a function of normalized thickness are shown in Figure 7. Results for representative ontogenetic and regenerated scales of fish maintained at 10°C are shown in Figure 7a and 7b, respectively. Despite some differences in the absolute mineral to collagen ratios among the individual scales, all the ontogenetic scales exhibited a distinct limiting layer, external elasmodine and the internal elasmodine (Figures 7a, 7c). The distributions and their transitions for ontogenetic scales of fish held at 10°C and 20°C fish were similar, with consistency in the normalized distances through the thickness of the scale where the transitions occur. By

comparison, the mineral/collagen ratios of the regenerated scales (Figures 7b, 7d) exhibited two characteristic regions that corresponded to the mineralized layer and basal layer. The maximum (i.e. peak) mineral content was lowest in the scales regenerated at 10°C (Fig. 7b).

Discussion

The scales of bony fishes represent a specialized class of dermal armor with a hierarchical structure of collagen fibers interwoven into mineralized layers of calcium-deficient apatite (Murcia et al., 2016). This architecture and the overlapping arrangement of scales on the skin surface not only enhances physical protection, but also enhances mobility by increasing flexibility and reducing hydrodynamic drag (Yang et al., 2013). Although the composition and mechanical behavior of fish scales have been well characterized in multiple species, information about whether these properties change when scales are regenerated and the effect that environmental temperature has on this process has not been elucidated. Rapid scale regeneration is an important survival trait in fish because it restores protection against potential predatory injury and the integrity of dermis for osmoregulation (Zydlewski et al., 2010; Olsen et al., 2012). Because temperature is the major rate controlling factor in this process, knowledge of how it affects the resulting form and function of regenerated scales can provide instructive information about the mechanisms that guide the assembly of biogenic structures and their utility for designing synthetic analogs.

In this investigation we characterized the microstructure and mechanical behavior of ontogenetic and regenerated scales from common carp held at water temperatures of 10° and 20°C. These temperatures approximate the mid-point and upper end of the range that carp encounter in the Columbia River basin (Figure 2a), yet were sufficiently different to elicit changes in structure, composition and response to mechanical stress between ontogenetic and regenerated scales.

Nevertheless, the mechanical properties of regenerated scales were generally inferior to those of ontogenetic scales, regardless of the rearing temperature. Strength and MOT, for example, were 60% and 70% lower, respectively, in regenerated compared to ontogenetic scales for the fish held at 10°C. For carp held at 20°C, the only property in regenerated scales that was not significantly lower than in ontogenetic scales was the elastic modulus. Moreover, regenerated scales did not have a well-defined limiting layer, nor a stratified elasmodine (consisting of external and internal elasmodine), but rather an outer mineralized layer and underlying basal layer. Although the mineral to collagen ratio was highest for the scales regenerated at 20°C, the mineralized layer occupied a larger portion of the total thickness for regenerated scales at 10°C due to the lower overall thickness of the scales. Overall, S and MOT were linearly related to the mineralization ratio (Figure 8).

If the primary purpose of scales is to provide protection from physical injury, microstructure development during regeneration should progress in a manner that prioritizes this function. Scale development starts in the dermis where fibroblasts accumulate and begin to construct the mineralized layer, which then evolves into the elasmodine (Bereiter-Hahn and Zylberberg, 1993). The mineralized layer grows preferentially in diameter, eventually extending across the full surface area of the scale. In teleost fish, elasmoblasts lining the bottom of the mineralized layer begin to deposit a layer of entangled mineralized collagen (Sire and Akimenko, 2004). Then, comparatively thick unidirectional layers (or plies) of non-mineralized collagen begin to generate at the base, establishing the basal layer, and increase the scale thickness as it grows in diameter. The limiting layer develops last and involves a slow accumulation of mineral on the top of the scale throughout the life of the fish (Sire, 1986).

We suggest that when scales are lost the highly mineralized limiting layer and external elasmodine should be preferentially synthesized from the regeneration process because they make the largest contribution to puncture resistance (Zhu et al., 2012). By contrast, although a thick collagen fiber bed is critical to toughness and tear resistance (Yang et al., 2014), we expected regeneration of this material would be prioritized less than the mineralized layers. Our results from measures of the layer topology, ply count and ply thickness showed that the regenerated scales in carp were composed of a single thick mineralized layer and plies of unidirectional collagen within the basal layer, which is consistent with previous work (Sire and Akimenko, 2004) and supports the suggestion that restoring physical protection is the proximate objective of the regeneration process. Whether carp scales organized the collagen within the mineralized layer into the serial unidirectional plies of the basal layer that become the foundation of the external elasmodine was unclear because we were not able to identify distinct collagen plies in this region by microscopic analysis. We expected to find mineralized plies of collagen in the basal layer because it is both stronger and tougher than non-mineralized collagen (Buehler, 2007) and would contribute to puncture resistance. There was also no clear demarcation between an external and internal elasmodine in the basal layer of the regenerated scales. However, based on Raman spectroscopy of the mineral/collagen ratio in the regenerated scales (Fig. 6 and Fig. 7), the ML is similar in normalized thickness (approx. 0.3) and mineral/collagen ratio (approx. 2 to 6) as the external elasmodine of the ontogenetic scales. Nevertheless, the mineralized layers of the regenerated scales in our study represented a lower proportion of the total scale thickness than the mineralized zone (i.e., limiting layer and external elasmodine) of the ontogenetic scales and may reflect partial balancing for toughness and flexibility while simultaneously advancing mineralization.

Comparison of the scales that regenerated at 10° and 20°C indicated that the water temperature had an important effect on mechanical behavior. Elastic modulus, S and MOT were all significantly lower in scales regenerated at 10° than at 20°C. Although BL and total thickness were approximately 50% greater in the regenerated scales of carp held at 20°C, the apparent difference was significant for the BL thickness ($p=0.047$) but total thickness did not reach the significance level of $p<0.05$ ($p=0.052$). For the thickness of individual plies in the elasmodine layers of scales regenerated at 10° and 20°C the difference is insignificant ($p \geq 0.133$). Hence, the basis for the differences in the mechanical properties of the regenerated scales at these temperatures appears to be unrelated to the microstructural features of the regenerated scales. However, Murcia et al., (2017) showed that S and E of the elasmodine layer increased with the ratio of external to internal elasmodine plies, which unfortunately could not be measured due to the lack of distinct external and internal elasmodine layers and absence of unidirectionally aligned plies of collagen fibrils in the regenerated scales. As an alternative, E, S, e_f and MOT can be expressed in terms of the degree of mineralization obtained by Raman spectroscopy and measured by the mineral/collagen ratio. The measures of mineral/collagen ratio in Figure 8 show the average values across the mineralized region of the scale. Other than e_f, the average mineral/collagen ratio for each of the other mechanical properties was higher in the regenerated scales from fish held at 20°C than at 10°C, and likely contributed to their superior tensile testing performance. The E of the scales should be closely correlated with mineralization since mineralized collagen and the limiting layer are stiffer (Beuhler, 2007; Arola et al., 2019). With the increased mineralization in the scales regenerated at 20°C, E nearly reached the same level as the ontogenetic scales. Also notable are the improvements with increasing mineralization for the S and MOT (Figure 8). Both

of these properties exhibited almost linear trend with the amount of mineralization, implying that mineral content has a marked role in the protection performance of the scales.

The results obtained from the compositional analysis of the scales mapped across the thickness using Raman spectroscopy further demonstrated that the maximum mineral/collagen ratio and the transition between the mineralized and non-mineralized layers differed between the regenerated scales of fish held at the two temperatures (Figure 7). For the scales regenerated at 10°C, the peak mineral content is lower than for the scales at 20°C. Furthermore, the spatial distribution in the mineral/collagen ratio of the scales regenerated at 20°C is highly consistent with the distribution in the ontogenetic scales at 20°C. Nevertheless, although the overall thickness of this highly mineralized region and the overall thickness of the regenerated scales was lower compared to the ontogenetic scales of fish held at 20°C, it would be interesting to determine if the regenerated scale morphology within individual fish would eventually converge to that of the ontogenetic scales, independent of temperature.

To the best of our knowledge, this is the first investigation of the structure-property relationships of both ontogenetic and regenerated fish scales obtained from the same fish. It is also the first assessment of the importance of temperature to the microstructure and mechanical properties of the regenerated scales. Despite its novelty, there are important limitations to the work that should be considered. First, the evaluation represents a snapshot of the structure and properties over the period of regeneration. According to their overall size (i.e. diameter), the regenerated scales had not reached confluence with the ontogenetic scales. Based on the lower thickness and absence of a well-defined limiting layer, the process of regeneration may not have been complete. Allowing the scales longer time to regenerate and assessing the microstructure at different stages of regeneration process could be informative. Our findings were also limited to the scales of six

different fish and only three at each temperature. Larger numbers of fish held at each temperature would increase confidence in our inferences related to the variation in structure, composition and mechanical behavior. Furthermore, our study only examined scales closest to the head region. Other investigations have shown that mechanical properties of scales vary spatially over the body of fish (Marino Cugno Garrano et al., 2012; Gil-Duran et al., 2016), which could be important in comparing the process of regeneration, as would the spatial sequence of scale development over the body. For many species, including carp, scale development follows a squamation process that occurs from the posterior to the anterior (Sire and Arnulf, 1990), and it would be of interest to determine if this processes similarly affects scale regeneration.

Finally, mature carp in the Colombia River and elsewhere have relatively few natural predators. They may be highly preyed upon as juveniles by fish species, and traits that evolve in response to selection pressures early in life (e.g. high levels of predation) can be expressed throughout the life of the organism. However, their functional role may diminish or even change. Thus, although the scales in large, mature carp still serve for physical protection, this may be less critical for survival than the scales of other fish where the likelihood of predation is high over a large part of their lifespan. The regeneration timeline of scales from other fish and the development of their microstructures through the regeneration process may be quite different. Investigating scale regeneration in other species could provide key insights to the processes governing material development for physical protection. This topic deserves more consideration and will be the focus of our future studies.

Summary

An experimental investigation was performed to characterize the microstructure of the ontogenetic and regenerated scales from the *Cyprinus carpio*, identify contributions to the mechanical properties of the scales and assess the importance of the environment in which they develop. Several fish were acquired wild from the Colombia River and then maintained live in an aquatic laboratory at either 10° or 20°C. Ontogenetic scales were extracted from the fish for analysis, as well as the regenerated scales after a period of development and growth. Results showed that the overall mechanical behavior of the regenerated scales was inferior to that of the ontogenetic scales regardless of the rearing temperature. The largest difference between the ontogenetic and regenerated scales was for the scales that regenerated at 10°C; the properties most affected were the strength and modulus of toughness, with differences of 60% and 70% with respect to the ontogenetic scales. For the fish held at 20°C, all properties were significantly different except for the elastic modulus. The regenerated scales did not exhibit a well-defined limiting layer, nor a stratified elasmodine (consisting of external and internal elasmodine), but rather an outer mineralized layer and underlying basal layer. While the mineral to collagen ratio was highest for the scales that regenerated at 20°C, the mineralized layer occupied a larger portion of the total thickness for scales that regenerated at 10°C. An assessment of all scales showed that the strength and toughness of the scales was linearly related to the mineralization ratio and that it appears that the mineralized layer is developed preferentially in regenerated scales to achieve the most effective protection during the growth process.

List of Symbols and Abbreviations

BL – Basal Layer

COV – Coefficient of Variation

E – Elastic Modulus

EE – External Elasmodine

e_f – Strain to failure

IE – Internal Elasmodine

LL – Limiting Layer

ML – Mineralized Layer

MOT – Modulus of Toughness

S - Strength

Acknowledgements

The authors gratefully acknowledge the contributions of Dr. Sandra Murcia (Intel) and Dr. Arun Devaraj (PNNL) for their fruitful discussions. The authors also acknowledge the University of Washington Biostatistics Department for the confirmation on statistical methods used in this study.

Competing Interests

The authors do not have any competing or conflicting interests to declare.

Funding

This research was supported in part by a seed grant from the University of Washington (Arola) and from a laboratory directed research and development fund associated with a Chemical Imaging Initiative at the Pacific Northwest National Laboratory (Linley). Part of this work was conducted at the Molecular Analysis Facility, a National Nanotechnology Coordinated Infrastructure site at the University of Washington which is supported in part by the National Science Foundation [grant ECC-1542101], the University of Washington, the Molecular Engineering & Sciences Institute, the Clean Energy Institute, and the National Institutes of Health.

References

Arola, D., Murcia, S., Stossel, M., Pahuja, R., Linley, T., Devaraj, A., Ramulu, M., Ossa, E. A. and Wang, J. (2018). The limiting layer of fish scales: structure and properties. *Acta Biomaterialia* **67**, 319–330.

Arola, D., Ghods, S., Son, C., Murcia, S. and Ossa, E. A. (2019). Interfibril hydrogen bonding improves the strain-rate response of natural armour. *Journal of The Royal Society Interface* **16**, 20180775.

Barthelat, F. (2007). Biomimetics for next generation materials. *Philosophical Transactions of the Royal Society A: Mathematical, Physical and Engineering Sciences* **365**, 2907–2919.

Bereiter-Hahn, J. and Zylberberg, L. (1993). Regeneration of teleost fish scale. *Comparative Biochemistry and Physiology Part A: Physiology* **105**, 625–641.

Bigi, A., Burghammer, M., Falconi, R., Koch, M. H. J., Panzavolta, S. and Riekel, C. (2001). Twisted plywood pattern of collagen fibrils in teleost scales: an x-ray diffraction investigation. *Journal of Structural Biology* **136**, 137–143.

Browning, A., Ortiz, C. and Boyce, M. C. (2013). Mechanics of composite elasmoid fish scale assemblies and their bioinspired analogues. *Journal of the Mechanical Behavior of Biomedical Materials* **19**, 75–86.

Bruet, B. J. F., Song, J., Boyce, M. C. and Ortiz, C. (2008). Materials design principles of ancient fish armour. *Nature Materials* **7**, 748–756.

Buehler, M. J. (2007). Molecular nanomechanics of nascent bone: fibrillar toughening by mineralization. *Nanotechnology* **18**, 295102.

Chen, P.-Y., Schirer, J., Simpson, A., Nay, R., Lin, Y.-S., Yang, W., Lopez, M. I., Li, J., Olevsky, E. A. and Meyers, M. A. (2012). Predation versus protection: fish teeth and scales evaluated by nanoindentation. *Journal of Materials Research* **27**, 100–112.

Currey, J. D. (1999). The design of mineralised hard tissues. *Journal of Experimental Biology* **202**, 3285–3294.

Duro-Royo, J., Zolotovsky, K., Mogas-Soldevila, L., Varshney, S., Oxman, N., Boyce, M. C. and Ortiz, C. (2015). MetaMesh: A hierarchical computational model for design and fabrication of biomimetic armored surfaces. *Computer-Aided Design* **60**, 14–27.

Gauldie, R. W., Coote, G., West, I. F., and Radtke, R. L.. (1990). The influence of temperature on the fluorine and calcium composition of fish scales. *Tissue and Cell* **22,** 645-654.

Ghods, S., Murcia, S., Ossa, E. A. and Arola, D. (2019). Designed for resistance to puncture: The dynamic response of fish scales. *Journal of the Mechanical Behavior of Biomedical Materials* **90**, 451–459.

Gil-Duran, S., Arola, D. and Ossa, E. A. (2016). Effect of chemical composition and microstructure on the mechanical behavior of fish scales from megalops atlanticus. *Journal of the Mechanical Behavior of Biomedical Materials* **56**, 134–145.

Giraud, M. M., Castanet, J., Meunier, F. J. and Bouligand, Y. (1978). The fibrous structure of coelacanth scales: A twisted 'plywood.' *Tissue and Cell* **10**, 671–686.

Goolish, E. M. and Adelman, I. R.. (1984). Effects of ration size and temperature on the growth of juvenile common carp (Cyprinus carpio L.). *Aquaculture* **36,** 27-35.

Guzzo, M. M., Mochnacz, N. J., Durhack, T., Kissinger, B. C., Killen, S. S. and Treberg, J. R. (2019). Effects of repeated daily acute heat challenge on the growth and metabolism of a cold water stenothermal fish. *J Exp Biol* **222**, jeb198143.

Ikoma, T., Kobayashi, H., Tanaka, J., Walsh, D. and Mann, S. (2003). Microstructure, mechanical, and biomimetic properties of fish scales from pagrus major. *Journal of Structural Biology* **142**, 327–333.

Jandt, K. D. (2008). Biological materials: fishing for compliance. *Nature Materials* **7**, 692–693.

Kardong, K. V. (2006). *Vertebrates: comparative anatomy, function, evolution*. McGraw-Hill New York.

Khayer Dastjerdi, A. and Barthelat, F. (2015). Teleost fish scales amongst the toughest collagenous materials. *Journal of the Mechanical Behavior of Biomedical Materials* **52**, 95–107.

Kloskowski, J. (2011). Impact of common carp Cyprinus carpio on aquatic communities: direct trophic effects versus habitat deterioration. *Fundamental and Applied Limnology/Archiv für Hydrobiologie* **178**245-255.

Liu, W., Chen, Z., Cheng, X., Wang, Y., Amankwa, A. R. and Xu, J. (2016a). Design and ballistic penetration of the ceramic composite armor. *Composites Part B: Engineering* **84**, 33–40.

Liu, P., Zhu, D., Yao, Y., Wang, J. and Bui, T. Q. (2016b). Numerical simulation of ballistic impact behavior of bio-inspired scale-like protection system. *Materials & Design* **99**, 201–210.

Liu, Z., Zhang, Z. and Ritchie, R. O. (2018). On the materials science of nature's arms race. *Advanced Materials* **30**, 1705220.

Marino Cugno Garrano, A., La Rosa, G., Zhang, D., Niu, L.-N., Tay, F. R., Majd, H. and Arola, D. (2012). On the mechanical behavior of scales from *cyprinus carpio*. *Journal of the Mechanical Behavior of Biomedical Materials* **7**, 17–29.

Martini, R. and Barthelat, F. (2016). Stretch-and-release fabrication, testing and optimization of a flexible ceramic armor inspired from fish scales. *Bioinspir. Biomim.* **11**, 066001.

Mayer, G. (2006). New classes of tough composite materials—lessons from natural rigid biological systems. *Materials Science and Engineering: C* **26**, 1261–1268.

Meyers, M. A., Chen, P.-Y., Lin, A. Y.-M. and Seki, Y. (2008). Biological materials: structure and mechanical properties. *Progress in Materials Science* **53**, 1–206.

Meyers, M. A., Lin, Y. S., Olevsky, E. A. and Chen, P.-Y. (2012). Battle in the amazon: arapaima versus piranha. *Advanced Engineering Materials* **14**, B279–B288.

Murcia, S. C. (2017). The natural armor of fish: an exploration of a biological composite. *PhD Thesis*, University of Washington, Seattle, WA.

Murcia, S., McConville, M., Li, G., Ossa, A. and Arola, D. (2015). Temperature effects on the fracture resistance of scales from *cyprinus carpio*. *Acta Biomaterialia* **14**, 154–163.

Murcia, S., Li, G., Yahyazadehfar, M., Sasser, M., Ossa, A. and Arola, D. (2016). Effects of polar solvents on the mechanical behavior of fish scales. *Materials Science and Engineering: C* **61**, 23–31.

Murcia, S., Lavoie, E., Linley, T., Devaraj, A., Ossa, E. A. and Arola, D. (2017). The natural armors of fish: A comparison of the lamination pattern and structure of scales. *Journal of the Mechanical Behavior of Biomedical Materials* **73**, 17–27.

Naleway, S. E., Porter, M. M., McKittrick, J. and Meyers, M. A. (2015). Structural design elements in biological materials: application to bioinspiration. *Advanced Materials* **27**, 5455–5476.

Panek, F.M. (1987). Biology and ecology of carp. In: Cooper, E.L. (ed.) Carp in North America. Bethesda, Md. American Fisheries Society. 1-16

Ohira, Y., Shimizu, M., Ura, K. and Takagi, Y. (2007). Scale regeneration and calcification in goldfish carassius auratus: quantitative and morphological processes. *Fisheries Science* **73**, 46–54.

Olsen, R.E., Oppedal, F., Tenningen, M. and Vold, A. (2012). Physiological response and mortality caused by scale loss in Atlantic herring. *Fisheries Research* **129**, 21-27.

Rudykh, S., Ortiz, C. and Boyce, M. C. (2015). Flexibility and protection by design: imbricated hybrid microstructures of bio-inspired armor. *Soft Matter* **11**, 2547–2554.

Sfakiotakis, M., Lane, D. M. and Davies, J. B. C. (1999). Review of fish swimming modes for aquatic locomotion. *IEEE J. Oceanic Eng.* **24**, 237–252.

Sire, J.-Y. and Akimenko, M.-A. (2004). Scale development in fish: a review, with description of sonic hedgehog (shh) expression in the zebrafish (Danio rerio). *The International Journal of Developmental Biology* **48**, 233–247.

Sire, J.-Y. and Arnulf, I. (1990). The development of squamation in four teleostean fishes with a survey of the literature. *Japanese Journal of Ichthyology* **37**, 11.

Sire, J.-Y. and Huysseune, A. (2003). Formation of dermal skeletal and dental tissues in fish: a comparative and evolutionary approach. *Biological Reviews* **78**, 219–249.

Song, J., Ortiz, C. and Boyce, M. C. (2011). Threat-protection mechanics of an armored fish. *Journal of the Mechanical Behavior of Biomedical Materials* **4**, 699–712.

Szewciw, L., Zhu, D. and Barthelat, F. (2017). The nonlinear flexural response of a whole teleost fish: contribution of scales and skin. *Journal of the Mechanical Behavior of Biomedical Materials* **76**, 97–103.

Yasuaki, T. Tetsuya, H. and Juro, Y. (1989) Scale regeneration of tilapia (Oreochromis niloticus) under various ambient and dietary calcium concentrations. *Comparative Biochemistry and Physiology Part A: Physiology* **92**: 605-608.

Thomas, K. Hansen, T., Brophy, D. Ó Maoiléidigh, N. and Fjelldal, P. G.. (2019). Experimental investigation of the effects of temperature and feeding regime on scale growth in Atlantic salmon Salmo salar post- smolts. *Journal of fish biology*

Torres, F. G., Troncoso, O. P., Nakamatsu, J., Grande, C. J. and Gómez, C. M. (2008). Characterization of the nanocomposite laminate structure occurring in fish scales from Arapaima Gigas. *Materials Science and Engineering: C* **28**, 1276–1283.

Torres, F. G., Malásquez, M. and Troncoso, O. P. (2015). Impact and fracture analysis of fish scales from arapaima gigas. *Materials Science and Engineering: C* **51**, 153–157.

Webb, P. W. (1983). Speed, acceleration and manoeuvrability of two teleost fishes. *Journal of Experimental Biology* **102**, 115–112.

Wegst, U. G. K., Bai, H., Saiz, E., Tomsia, A. P. and Ritchie, R. O. (2015). Bioinspired structural materials. *Nature Materials* **14**, 23–36.

Weiner, S. and Addadi, L. (1997). Design strategies in mineralized biological materials. *J. Mater. Chem.* **7**, 689–702.

Yang, W., Chen, I. H., Gludovatz, B., Zimmermann, E. A., Ritchie, R. O. and Meyers, M. A. (2013). Natural flexible dermal armor. *Advanced Materials* **25**, 31–48.

Yang, W., Sherman, V. R., Gludovatz, B., Mackey, M., Zimmermann, E. A., Chang, E. H., Schaible, E., Qin, Z., Buehler, M. J., Ritchie, R. O., et al. (2014). Protective role of arapaima gigas fish scales: structure and mechanical behavior. *Acta Biomaterialia* **10**, 3599–3614.

Yang, W., Meyers, M. A. and Ritchie, R. O. (2019). Structural architectures with toughening mechanisms in nature: a review of the materials science of Type-I collagenous materials. *Progress in Materials Science* **103**, 425–483.

Zhang, Z., Zhang, Y.-W. and Gao, H. (2011). On optimal hierarchy of load-bearing biological materials. *Proc. R. Soc. B* **278**, 519–525.

Zhu, D., Ortega, C. F., Motamedi, R., Szewciw, L., Vernerey, F. and Barthelat, F. (2012). Structure and mechanical P=performance of a "modern" fish scale. *Advanced Engineering Materials* **14**, B185–B194.

Zhu, D., Szewciw, L., Vernerey, F. and Barthelat, F. (2013). Puncture resistance of the scaled skin from striped bass: collective mechanisms and inspiration for new flexible armor designs. *Journal of the Mechanical Behavior of Biomedical Materials* **24**, 30–40.

Zimmermann, E. A., Gludovatz, B., Schaible, E., Dave, N. K. N., Yang, W., Meyers, M. A. and Ritchie, R. O. (2013). Mechanical adaptability of the bouligand-type structure in natural dermal armour. *Nature Communications* **4**, 2634.

Zydlewski, J., Zydlewski, G. and Danner, G.R. (2010). Descaling injury impairs the osmoregulatory ability of Atlantic salmon smolts entering seawater. *Transactions of the American Fisheries Society* **139(1)**,129-136.

Figures

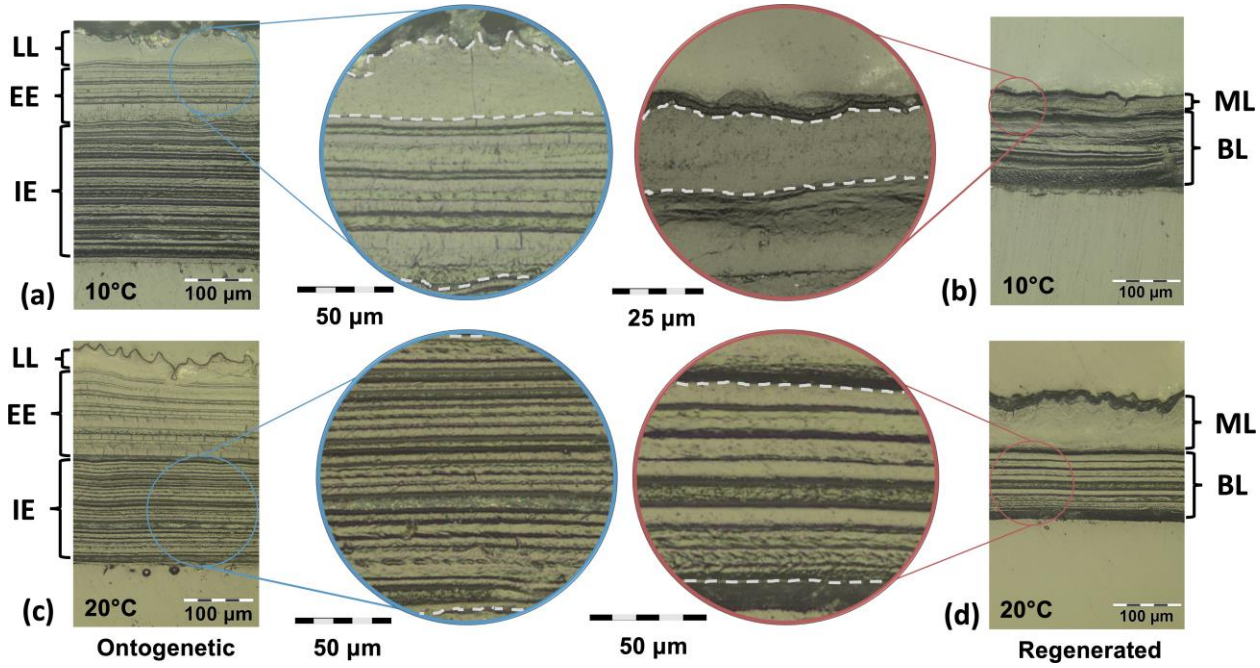

Figure 1 Microstructure of representative scales from the a) 10°C Ontogenetic (10-O), b) 10°C Regenerated (10-R) , c) 20°C Ontogenetic (20-O), and d) 20°C Regenerated (20-R) groups, respectively. White dashed lines indicate the borders of microstructural regions highlighted in the higher magnification micrographs.

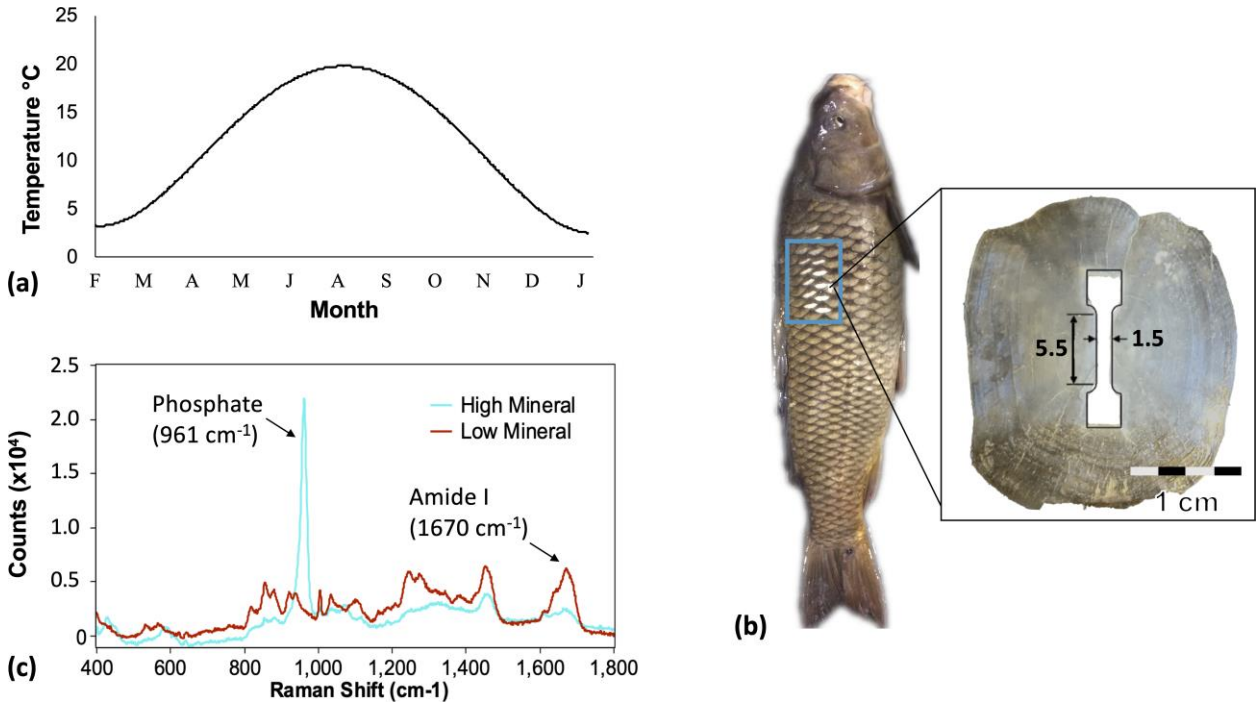

Figure 2 Schematic descriptions for specimen preparation and evaluation. (a) approximation of the annual temperature cycle (2017 – 2018) for the Columbia River at the PNNL Aquatic Research Laboratory. The line was fit to the mean monthly temperatures by least squares regression. (b) Sectioning of the tensile specimens and location for microstructure evaluation. (c) Representative Raman spectrum with labeling of the phosphate and amide I peak indicated at 961 and 1690 cm-1, respectively.

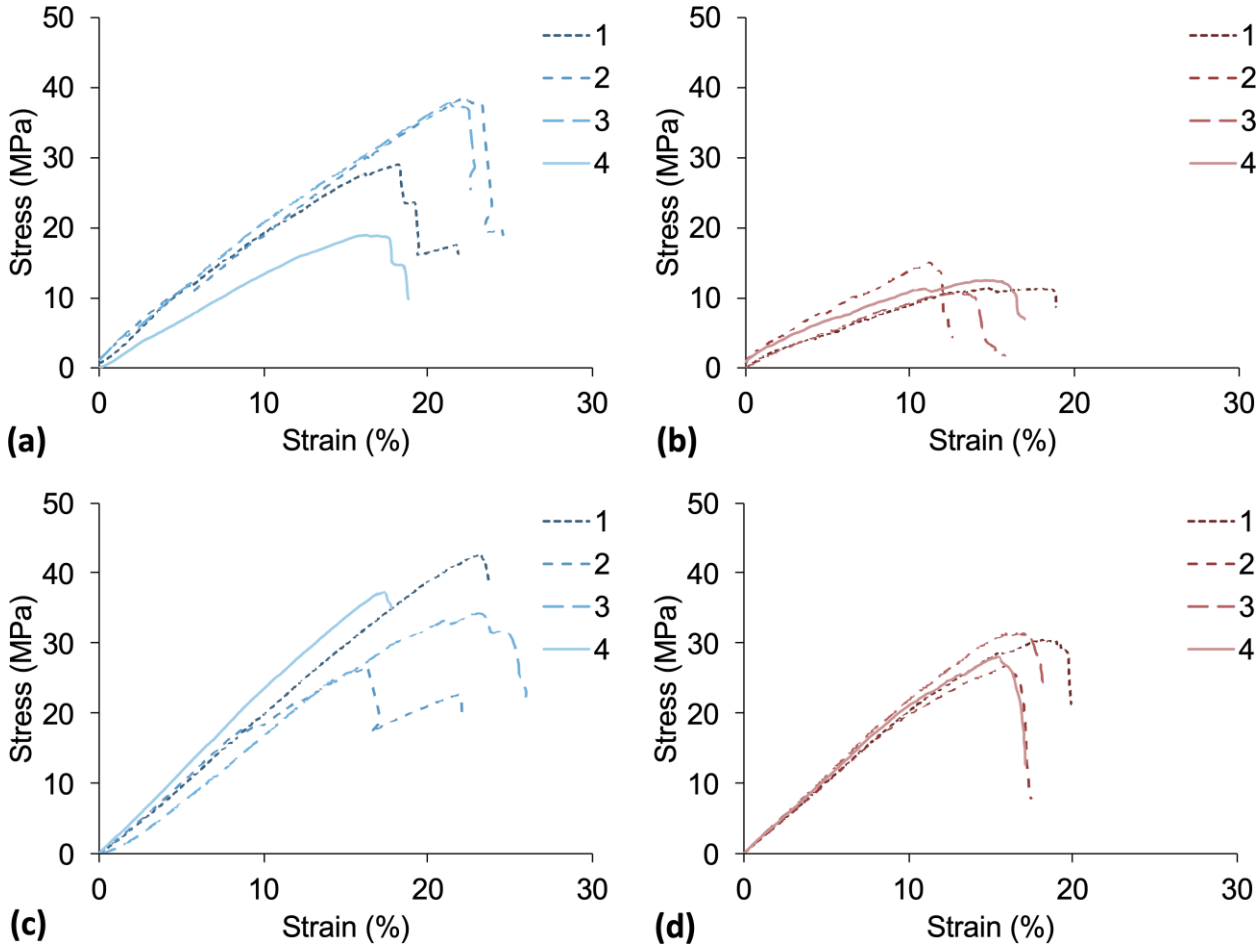

Figure 3 Stress-strain curves for scales from two different fish. One fish (Fish A) at 10 °C (a) ontogenetic and (b) regenerated scales. Another fish (Fish D) at 20 °C (c) original and (d) regenerated scales.

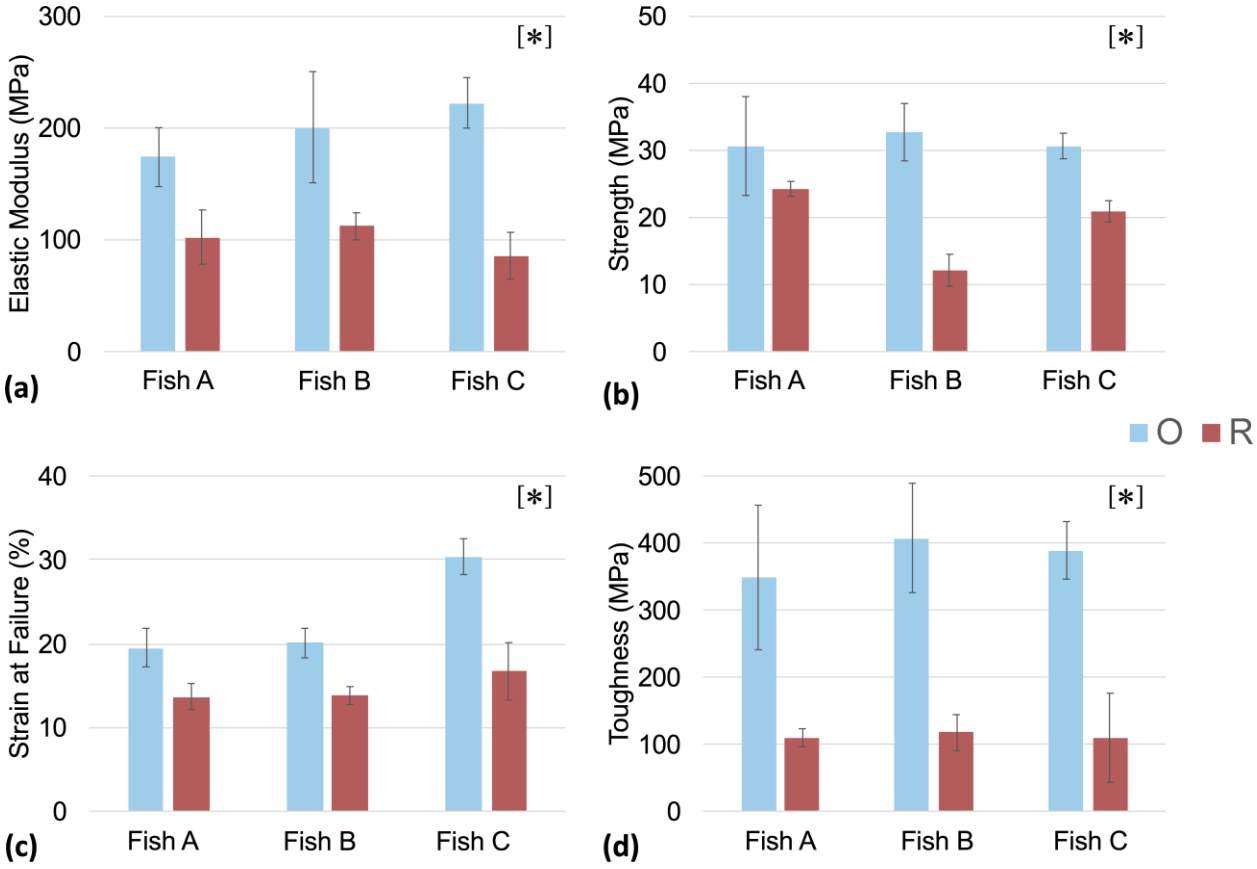

Figure 4 Tensile properties of the ontogenetic (O) and regenerated (R) scales for fish maintained at 10 °C. (a) Elastic modulus, (b) Strength, (c) Strain at Failure, and (d) Toughness. The results presented in each column represent the average and standard deviation of four tensile tests. The [*] in the upper right of this figure indicates a significant difference ($p \leq 0.05$) for O vs. R of that metric.

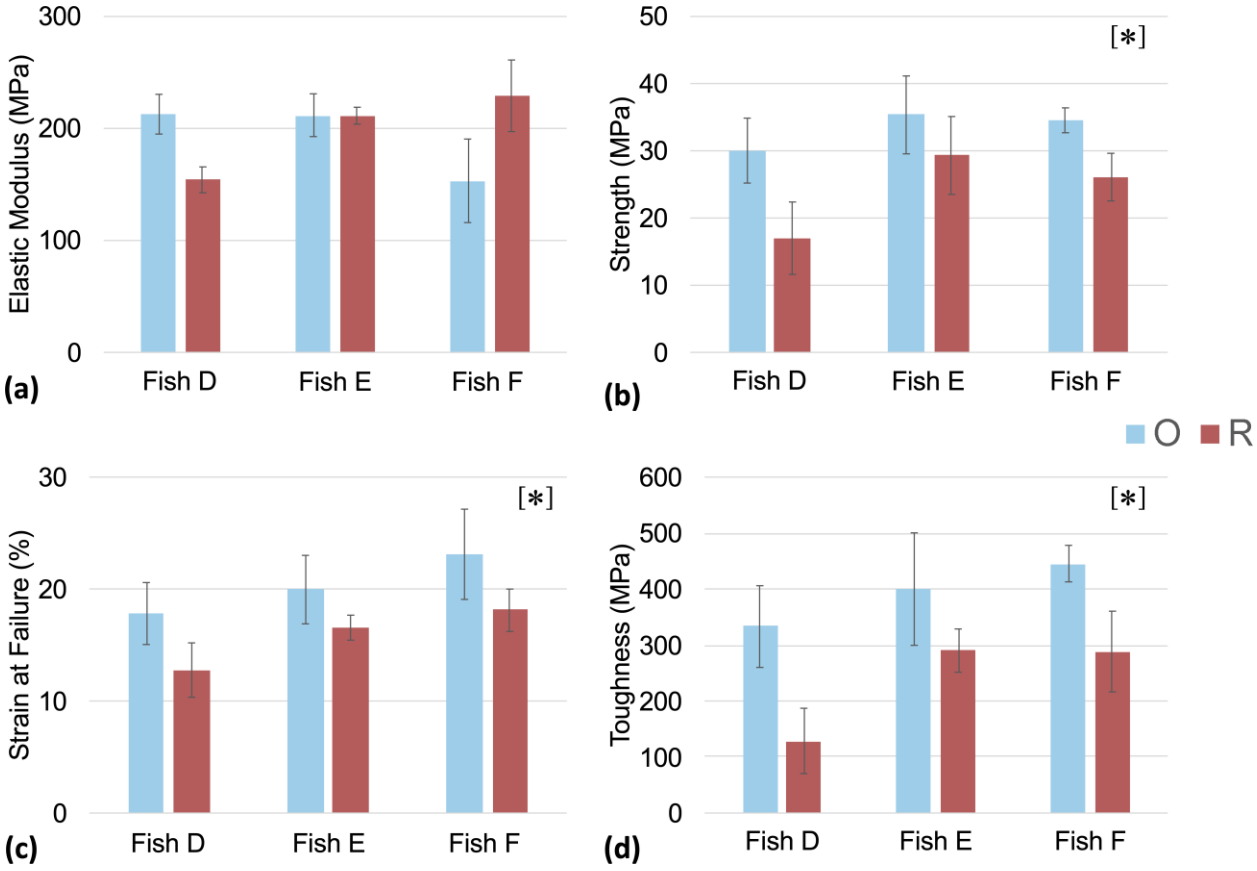

Figure 5 Tensile properties of ontogenetic (O) and regenerated (R) scales for fish maintained at 20 °C. (a) Elastic modulus, (b) Strength, (c) Strain at Failure, and (d) Toughness. The results presented in each column represent the average and standard deviation of four tensile tests. The [*] in the upper right of this figure indicates a significant difference ($p \leq 0.05$) for O vs. R of that metric.

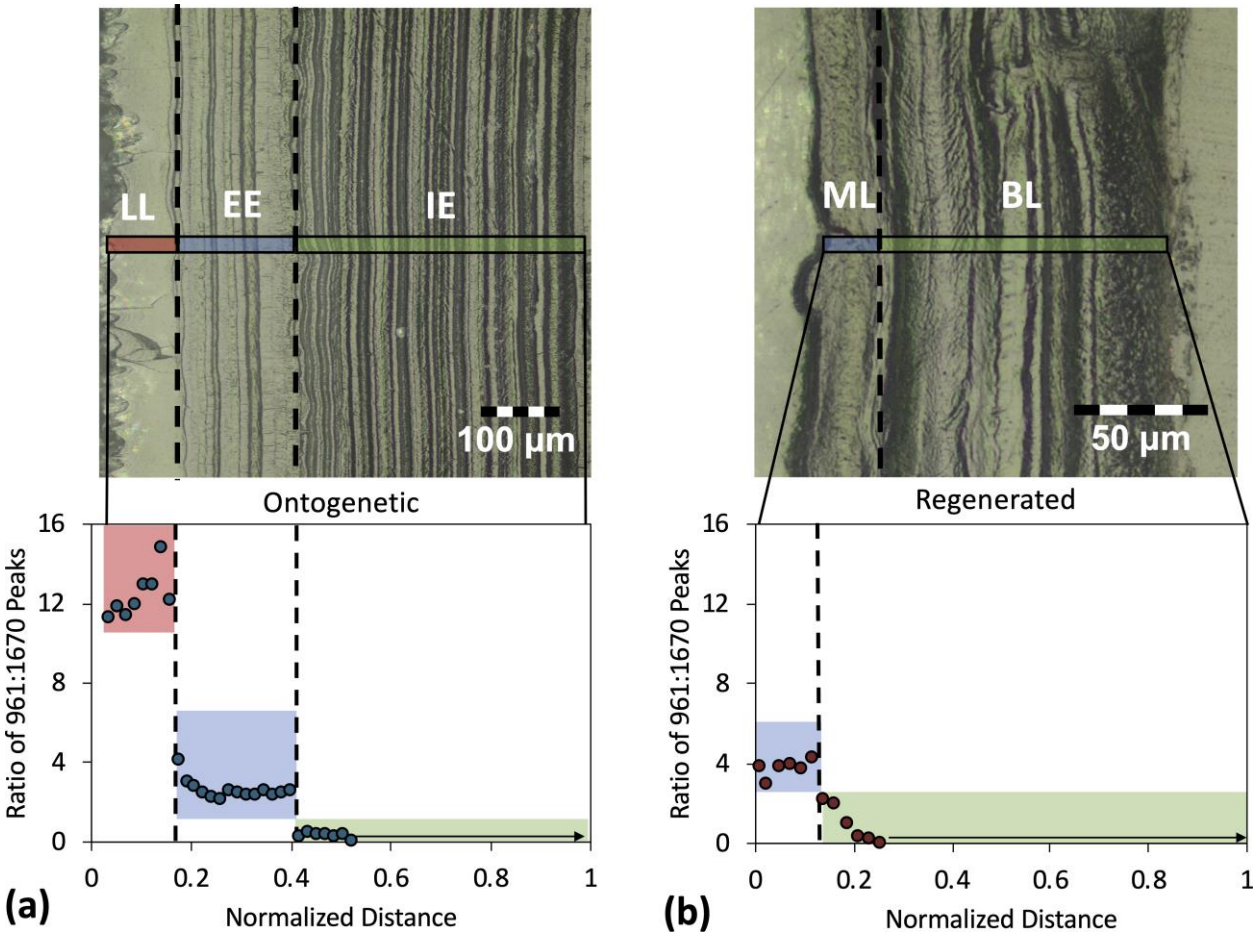

Figure 6 Micrographs representing cross-sections and composition of the (a) ontogenetic and (b) regenerated scales. The exterior is on the left and the important regions of the scales are highlighted. The Limiting Layer (LL), External Elasmodine (EE), and Internal Elasmodine (IE) are highlighted for the ontogenetic scales whereas the Mineralized layer (ML) and Basal layer (BL) are indicated tor the regenerated scale. The mineral/collagen ratio for these regions are shown as obtained from Raman spectroscopy.

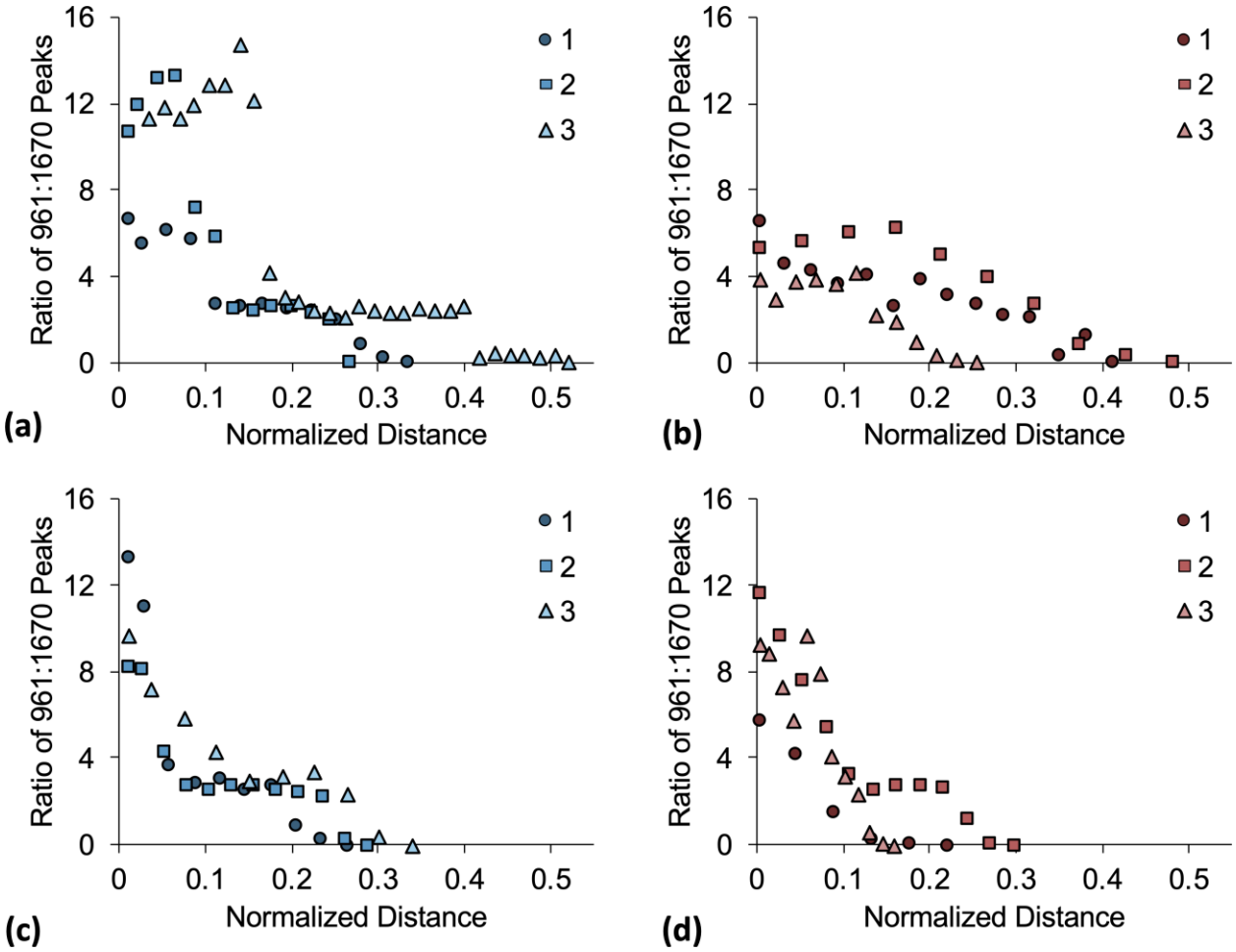

Figure 7 Mineral to collagen ratios presented as a function of distance from the outer surface through the thickness of representative scales normalized by the total thickness of the scale. Shown are results for three scales from Fish A maintained at 10°C, (a) ontogenetic and (b) regenerated and Fish D maintained at 20°C, (c) ontogenetic and (d) regenerated.

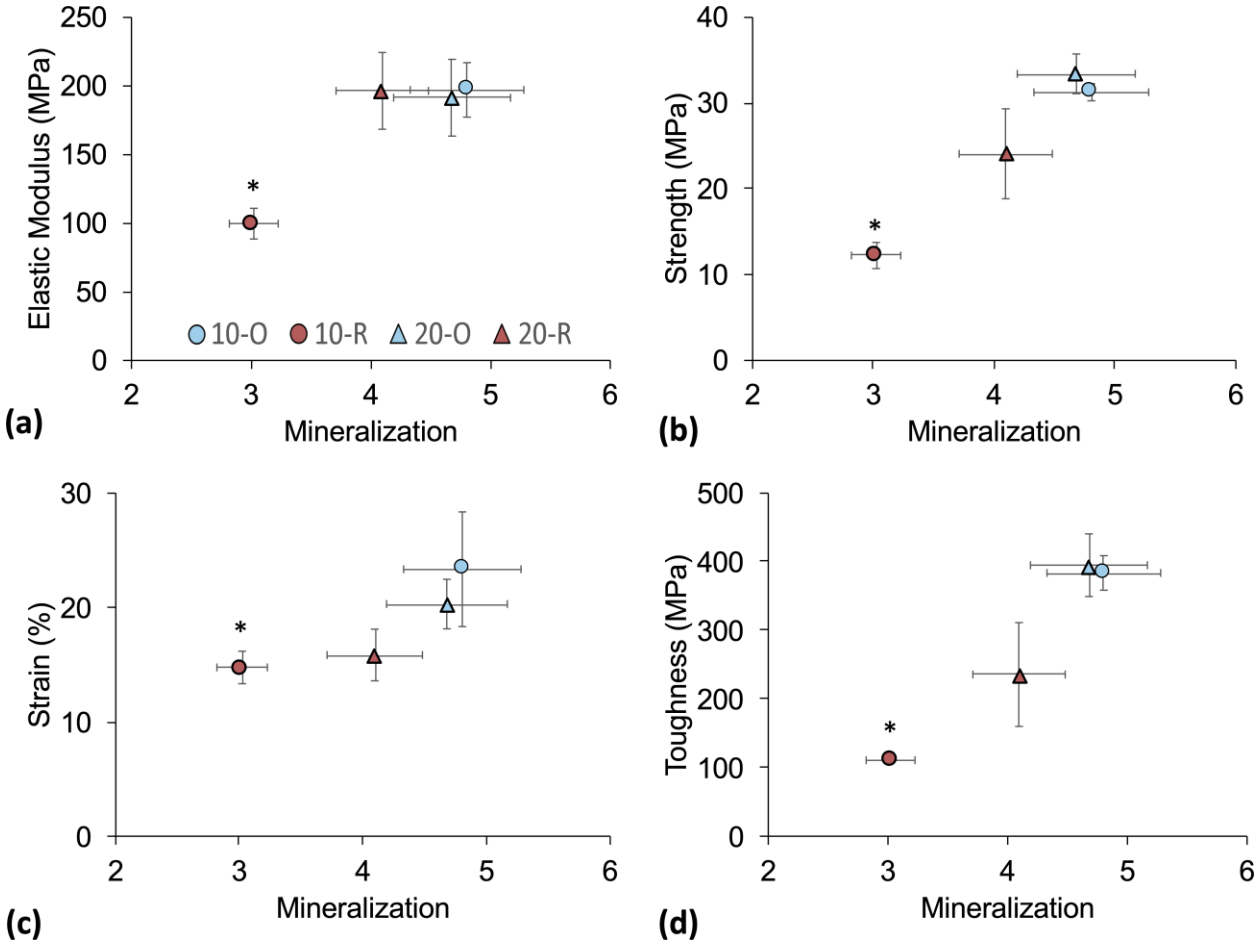

Figure 8 Relationship between mechanical properties and degree of mineralization (average mineral/collagen ratio within the mineralized region – EE or ML) for the ontogenetic (O) and regenerated (R) scales for fish from both the 10° and 20°C environments. (a) Elastic modulus, (b) Strength, (c) Strain at Failure, and (d) Toughness. All data is shown in terms of the average and standard deviation. The * indicates that the group's mineralization is significantly different ($p \leq 0.05$) from the others.

Table 1 Comparison of the ontogenetic and regenerated scale morphology. LL, EE and IE refer to the limiting layer, external elasmodine and internal elasmodine, respectively of the ontogenetic scales. ML and BL refer to the mineralized layer and basal layer, respectively of the regenerated scales. The data consists of specimens (4) from each fish (3) maintained at each of the two water temperatures (10 and 20°C), for a total of 24 experiments (4x2x3 = 24) for the ontogenetric and regenerated conditions All data is presented as the mean with the standard error in parenthesis.

	Layer Thickness (μm)					Number of Plies		
	LL	EE	ML	IE	BL	**Total**	EE	IE	BL
10-O	48 (5)	103 (6)		223 (16)		374 (19)	13 (0.8)	30 (3.0)	
10-R			49* (7)		103* (6)	152* (12)			10* (0.5)
20-O	53 (4)	96 (8)		204 (24)		353 (20)	9 (1.2)	28 (3.6)	
20-R			50* (3)		157* (31)	207* (34)			13* (1.6)

* indicates $p<0.001$ between ontogenetic and regenerated groups at same temperature